

RESEARCH ARTICLE

10.1029/2017JD028212

Current and Future Estimates of Wind Energy Potential Over Saudi Arabia

Wanfang Chen¹, Stefano Castruccio², Marc G. Genton¹, and Paola Crippa³

¹Statistics Program, King Abdullah University of Science and Technology, Thuwal, Saudi Arabia, ²Department of Applied and Computational Mathematics and Statistics, University of Notre Dame, Notre Dame, IN, USA, ³Department of Civil and Environmental Engineering and Earth Sciences, University of Notre Dame, Notre Dame, IN, USA

Key Points:

- Performance of five MENA CORDEX runs in simulating wind speed spatiotemporal variabilities is assessed against reanalysis data
- MENA CORDEX runs with the highest skills are used to quantify the wind energy potential in Saudi Arabia for current and future climates
- Regions and months or seasons with high wind energy potential for current and future climates are identified

Supporting Information:

- Supporting Information S1

Correspondence to:

P. Crippa,
pcrippa@nd.edu

Citation:

Chen, W., Castruccio, S., Genton, M. G., & Crippa, P. (2018). Current and Future Estimates of Wind Energy Potential Over Saudi Arabia. *Journal of Geophysical Research: Atmospheres*, 123, 6443–6459. <https://doi.org/10.1029/2017JD028212>

Received 19 DEC 2017

Accepted 18 MAY 2018

Accepted article online 24 MAY 2018

Published online 28 JUN 2018

Abstract Saudi Arabia has a long tradition of relying on fossil fuels for satisfying its energy demand. With the rising energy needs due to population growth and societal development, the nation is seeking other sources of energy, which include its largely underused wind resources. In this paper, we analyze the wind power potential in Saudi Arabia based on the MENA CORDEX (Middle East North Africa Coordinated Regional Climate Downscaling Experiment) model output. We investigate which climate settings and MENA CORDEX runs best capture the spatiotemporal patterns of reanalysis products, as assessed by multiple statistical metrics. Although there is a systematic negative bias in wind speed magnitudes for the five analyzed MENA CORDEX simulations, all runs are able to reproduce the seasonality and annual cycle of wind speed shown in the reanalysis data. The MENA CORDEX run with the highest skills is used to quantify the wind energy potential in Saudi Arabia in both current and future climates. Our analysis shows that a high wind energy potential exists over a vast area of western Saudi Arabia, particularly in the region between Medina and the Red Sea coast and during summer months. Based on model projections, the energy potential in these areas is likely to persist at least until the middle of the 21st century and thus may provide a valuable renewable source of energy.

1. Introduction

Investigating the spatial and temporal variabilities of near-surface wind speed is critical to understand the historical evolution and variation of wind climatology, as well as to make future projections in a warming world (Pryor et al., 2005; Rasmussen et al., 2011). Moreover, characterizing wind speed spatiotemporal patterns is crucial to assess the associated energy potential and thus to develop infrastructures in regions where these resources are most abundant. Global or regional wind climatology, extremes, and wind energy potential have been mostly inferred from Earth System Model (ESM) ensembles and regional climate model (RCM) experiments. For example, Lu et al. (2009) integrated direct observations of wind speeds and profiles (when-ever available) into the Goddard Earth Observing System Data Assimilation System ESM that run globally at a spatial resolution of $0.50^\circ \times 0.67^\circ$ (latitude \times longitude) for a specific year of interest. However, their estimates and model performance were not evaluated against observations. Zhou et al. (2012) estimated the energy potential of global onshore wind using the Climate Forecast System Reanalysis data from the National Centers for Environmental Prediction (Saha et al., 2010), available at higher spatial resolution (0.31° latitude/longitude) for the years 1980–2009. Lu et al. (2009) provided improved quantification of global wind energy potential, but their estimates are negatively biased in comparison with those derived from high-resolution data sets (New et al., 2002) or regional model simulations (Pryor, Barthelmie, & Schoof, 2012), which more accurately capture regional variabilities and thus provide insights about where to harvest the highest wind speeds.

Saudi Arabia has mostly relied on fossil fuels for its energy needs, but this is changing due to the rising demand in energy resulting from industrial development, urbanization, and growth of its population. Saudi Arabia has a very large underused potential of renewable energy, and it is planning to build a capacity of 54 GW by 2032, of which 9 GW are expected to come from wind power (KA-CARE, 2012). Due to the country's sparse and difficult access to data from monitoring stations, most studies evaluating Saudi Arabia's wind potential have focused on a few locations only, including five coastal sites (Rehman & Ahmad, 2004), and a few others in the Rafha area (Rehman et al., 2007) and the western province of Saudi Arabia (Shaahid et al., 2014). To overcome the challenge associated with the observational spatial and temporal coverage, Yip et al. (2016) assessed

the wind energy potential over the Arabian Peninsula during the period 1979–2014 using data from the Modern Era Retrospective-Analysis for Research and Applications (MERRA, Rienecker et al., 2011) data set, which has a spatial resolution of $0.5^\circ \times 0.67^\circ$ (latitude \times longitude). They found more abundant wind resources over the western mountains than most of the coastal areas of the Red Sea, as well as persistent winds along the Arabian Gulf coasts.

The international Coordinated Regional Climate Downscaling Experiment (CORDEX, Jones et al., 2011), sponsored by the World Climate Research Program, is responsible for the global coordination of regional climate downscaling to improve regional climate change adaptation and impact assessment. In this work, we focus on the Middle East North Africa (MENA) CORDEX Program, which is a branch of the CORDEX initiative and includes the Arabian Peninsula, the focus area of our research. Our objectives are the following:

1. to investigate the spatiotemporal patterns of near-surface wind speeds for current climate conditions (years 1980–2005) based on the MENA CORDEX output,
2. to investigate the sources of variability in wind speed resources relative to multiple reanalysis products, and
3. to quantify wind power density (WPD) and associated spatiotemporal patterns for current and future climates.

We evaluate the degree of agreement between climate model outputs and reanalysis data by computing multiple statistical metrics, including wind speed magnitudes (means and quantiles), historical trends, return periods, temporal (interannual and intra-annual) variabilities, spatial patterns, extremal behavior, and multi-decadal future trends. Discrepancies between simulated and reanalysis wind speed patterns are investigated by comparing the skills of different MENA CORDEX ensemble members as a function of spatial resolution and initial/lateral boundary conditions.

The paper is organized as follows. In section 2, we describe the wind data from MENA CORDEX and the reanalysis products, as well as the preprocessing required to homogenize the spatial and temporal resolution of the analyzed data sets. In section 3, we introduce the statistical metrics and methods used to assess model performance and define WPD. In sections 4–6, we assess the performance of the five MENA CORDEX runs in simulating wind speeds over Saudi Arabia relative to the reanalyses. The statistical metrics are computed to investigate the spatially averaged annual cycle/seasonality, temporal variabilities, spatial fields of the mean, standard deviation, quantiles and return levels of wind speeds, and wind speed variabilities over six regions in Saudi Arabia. In section 7, we quantify the wind energy potential, by computing WPD from both MERRA-2 and the MENA CORDEX run with highest performance. We then investigate possible sources of model bias (section 8), draw some conclusions, and discuss future wind energy potential scenarios in section 9.

2. Data

In this study, we focus on the Arabian Peninsula, bounded approximately by longitudes 34°E – 56°E and latitudes 16°N – 33°N . The domain of our study also includes the Red Sea, the Persian Gulf, parts of the Arabian Sea, Iraq, Iran, Egypt, and Sudan. We investigate the daily 2-D near-surface (i.e., 10 m above surface) wind speed using the five simulated historical runs performed by the Swedish Meteorological and Hydrological Institute, from the publicly available MENA CORDEX data set published via the Earth System Grid Federation. The historical ensemble runs are ESM-driven simulations forced with data from the Coupled Model Intercomparison Project (Taylor et al., 2012) historical experiments. We also analyze wind speed projections from the two CORDEX runs with the highest skills in capturing spatiotemporal variability of reanalysis data. Both runs adopt the Representative Concentration Pathways 8.5 scenario until 2100 (van Vuuren et al., 2011). In addition, in order to investigate the effect of lateral boundary conditions on model bias and variability in the historical MENA CORDEX runs, we perform an additional comparison against two MENA CORDEX runs forced by ERA-Interim (Dee et al., 2011).

Since direct observations of wind speed over Saudi Arabia are sparse and not publicly available (Yip et al., 2016), we consider the recently released version 2 of MERRA (i.e., MERRA-2, Gelaro et al., 2017) reanalysis data set as the “reference” for comparison with MENA CORDEX. MERRA was a product of National Aeronautics and Space Administration’s Global Modeling and Assimilation Office, which placed observations from its Earth Observing System satellites into climate context, and MERRA-2 was recently introduced to replace the MERRA data set, in response to the advances made in the assimilation system. Further, we perform an additional

Table 1

Key Characteristics of the MENA CORDEX Simulations, MERRA-2, and ERA-Interim Reanalysis Products Used in This Study

Model run	Driving experiment	Spatial resolution (latitude×longitude)	Temporal resolution	Years	Driving model	Institute
CORDEX-1	historical	0.44° × 0.44°	daily	1950–2005	CNRM-CM5	CNRM-CERFACS
CORDEX-2	historical	0.44° × 0.44°	daily	1950–2005	EC-EARTH	ICHEC
CORDEX-3	historical	0.44° × 0.44°	daily	1950–2005	GFDL-ESM2M	NOAA-GFDL
CORDEX-4	historical	0.22° × 0.22°	daily	1950–2005	GFDL-ESM2M	NOAA-GFDL
CORDEX-5	historical	0.22° × 0.22°	daily	1950–2005	EC-EARTH	ICHEC
CORDEX22	evaluation	0.22° × 0.22°	daily	1980–2010	ERAINT	ECMWF
CORDEX44	evaluation	0.44° × 0.44°	daily	1980–2010	ERAINT	ECMWF
CORDEX-2	rcp85	0.44° × 0.44°	daily	2006–2100	EC-EARTH	ICHEC
CORDEX-4	rcp85	0.22° × 0.22°	daily	2006–2100	GFDL-ESM2M	NOAA-GFDL
MERRA-2	historical	0.50° × 0.625°	hourly	1979–2017	reanalysis	NASA-GMAO
ERA-Interim	historical	0.75° × 0.75°	6-hourly	1979–2017	reanalysis	ECMWF

Note. ECMWF = European Centre for Medium-Range Weather Forecasts; GMAO = Global Modeling and Assimilation Office; ICHEC = Irish Centre for High-End Computing; NASA = National Aeronautics and Space Administration; NOAA = National Oceanic and Atmospheric Administration; CORDEX = Coordinated Regional Climate Downscaling Experiment; MERRA-2 = Modern Era Retrospective-Analysis for Research and Applications version 2.

evaluation relative to the ERA-Interim reanalysis produced by European Centre for Medium-Range Weather Forecasts to investigate the presence of a possible regional bias in the MERRA-2 data set.

Table 1 summarizes the key characteristics of the data sets used in our study. The last two columns of Table 1 indicate the ESMs providing initial and lateral boundary conditions for each MENA CORDEX run, and the institutes producing those ESMs, respectively. All of the nine MENA CORDEX runs analyzed are based on the same RCM, that is, the Rossby Centre regional atmospheric model (RCA4, Kupiainen et al. (2011)); thus, differences in model output are dictated by the different spatial resolution at which RCA4 is applied and to the different lateral boundary conditions.

Since only hourly U (zonal velocity) and V (meridional velocity) wind speed components at 10 m above the displacement height (U_{10M} and V_{10M} , respectively) are available from the 2-D atmospheric single-level diagnostics MERRA-2 files, we reconstruct the near-surface wind speed as

$$10 \text{ m wind speed} = \sqrt{U_{10M}^2 + V_{10M}^2}. \quad (1)$$

We then compute the MERRA-2 daily average winds from hourly wind speeds. For consistency, we also reconstruct the daily near-surface wind speeds from ERA-Interim and MENA CORDEX based on the U and V components. In this study, we focus on onshore winds; thus, all statistical metrics reported are computed based on land areas only.

In this study, we focus on the 1 January 1980 to 31 December 2005 period (26 years), which is the overlapping period between the MENA CORDEX, MERRA-2, and ERA-Interim data sets. Spatial fields of reconstructed wind speed from MENA CORDEX runs with a spatial resolution of $0.22^\circ \times 0.22^\circ$ or $0.44^\circ \times 0.44^\circ$ are interpolated to a common $0.50^\circ \times 0.625^\circ$ (latitude×longitude) grid to match the one used in MERRA-2 by applying a simple neighborhood-averaging method. Analogous methods are used for regridding data from CORDEX to ERA-Interim spatial resolution to evaluate model runs against that reanalysis product. The final data consist of $35 \times 35 = 1,225$ spatial locations in MERRA-2 spatial resolution and $31 \times 24 = 744$ locations in ERA-Interim spatial resolution, over a period of 9,497 days.

In order to examine the wind spatial variability over regions with different topographies and high-energy potentials, we focus on six circular regions (referred to as R1–R6, Figure 1) with a radius of 1° latitude/longitude, similar to those proposed in Tagle et al. (2017). The elevation data are retrieved from Google Maps Elevation application programming interface (Google Developers, 2017). Region 1 (R1) is located between Tabuk and Yanbu, whereas Region 3 (R3) is located between Yanbu and Mecca; both regions are close to the Red Sea. Region 2 (R2), in the north, comprises the city of Sakaka; Region 4 (R4) is close to the city of Wadi ad-Dawasir, east of the Asir Mountains; Region 5 (R5) is on a flatland in the southern part of Riyadh; Region 6

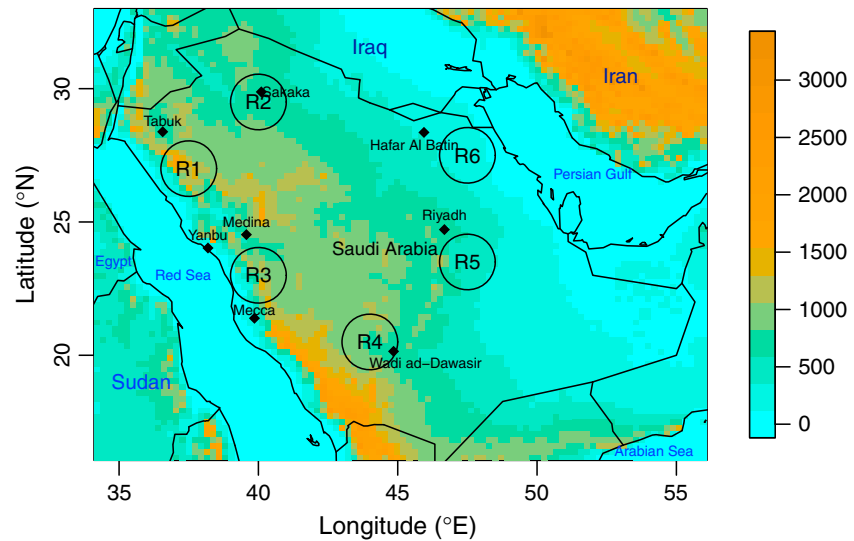


Figure 1. Analyzed domain and location of the six regions (i.e., R1–R6) in Saudi Arabia. The color shading indicates terrain elevation (in meters).

(R6) is in the northeast and close to the Persian Gulf. The far eastern part of Saudi Arabia is not represented within the region selection because of the substantially lower wind speeds over that area throughout the year from both MERRA-2 and CORDEX. Given that major interest is in areas of high-energy potentials, that part of Saudi Arabia is discarded from further analyses.

3. Methods

In this section, we illustrate some of the methods and metrics used in our research.

3.1. Taylor Diagram

The Taylor diagram (Taylor, 2001) is a graphical tool designed to summarize the following three statistical metrics used to quantify the similarity in spatial patterns between model simulations and direct observations (or a reference): (1) the Pearson correlation, (2) the standard deviation, and (3) the root-mean-square difference (RMSD). The Taylor diagram has been widely used to provide a comparative assessment of climate models in simulating global climate in relation to observational data (Chen et al., 2012; Ebert et al., 2007; Gleckler et al., 2008; Haidvogel et al., 2008; Pryor, Barthelmie, & Schoof, 2012; Schmidt et al., 2006). Specifically, in the Taylor diagram, the Pearson correlation coefficient is represented by the azimuthal angle, the ratio of standard deviations by the radial distance from the origin, and the RMSD is proportional to the distance to a reference point on the x axis where the ratio of the standard deviations is equal to 1 (Taylor, 2001). Model simulations that lie closest to this reference point on the x axis have the highest degree of agreement with the reference data, since they have a high correlation, a similar standard deviation and a low RMSD relative to observations.

In this study, we use the Taylor diagram to visually display the similarities of the five MENA CORDEX simulations in relation to a reference reanalysis based on the three aforementioned statistical metrics. Model performances are assessed in terms of temporal trends such as the spatially averaged monthly mean wind speeds, (section 4), spatial patterns (section 5), and spatiotemporal patterns (section 6) of wind speeds.

3.2. Functional Boxplots

The functional boxplot (Sun & Genton, 2011), an extension of the classical boxplot, is an informative exploratory tool for visualizing data that continuously vary in space and time. The classical boxplot can be created by simply ordering one-dimensional observations from the smallest to the largest value. For functional data, each observation is a function (e.g., a curve or an image), and all the observations are center-outward ordered based on the concept of band depth (López-Pintado & Romo, 2009) or other notions of depth. Based on the ranking, a functional boxplot is able to display three descriptive statistics: the median curve, the envelope of the 50% central region, and the maximum nonoutlying envelope (Sun & Genton, 2011). Outliers are detected as exceeding 1.5 times the 50% central region, similar to classical boxplots.

In this study, we use functional boxplots to compare the spatiotemporal wind speed and WPD patterns from both MENA CORDEX and MERRA-2, for current or future periods over the six selected regions introduced in section 2.

3.3. Return Levels

High-speed near-surface winds can be destructive to the integrity of infrastructures (e.g., the electricity distribution networks). Therefore, an accurate assessment of extreme wind speeds is crucial for engineering and risk management purposes (Cook, 1986; Kunz et al., 2010). In this study, we estimate the extreme wind speeds from both MENA CORDEX and MERRA-2 based on the M -year return level, defined as an extreme event that, on average, occurs once every M years. A detailed review of this method based on Davison and Smith (1990) is included in the supporting information. To avoid modeling complex spatiotemporal (seasonal) patterns, we restrict our attention to the three summer months, that is, June, July, and August (JJA), characterized by the strongest wind regimes of the year.

3.4. Wind Power Density

The WPD is an important measure for assessing the potential of wind energy (Emeis, 2013). It is defined as

$$\text{WPD} = \frac{1}{2} \rho w^3, \quad (2)$$

where w is the wind speed at a given measurement height or adjusted-to-hub height (i.e., the traditional turbine operational height that we assume to be 80 m), and ρ is the air density. WPD is a measurement of the wind power that is available per unit turbine area. There are several methods commonly used to extrapolate near-surface wind speed measurements to the hub height. One is to use the power law method (Emeis, 2005), which assumes that wind speed at a certain height z is approximated by

$$w(z) = w(z_r) \left(\frac{z}{z_r} \right)^\alpha, \quad (3)$$

where z_r is the reference height, $w(z_r)$ is the wind speed at z_r , and α is the power law exponent. In our case, we use the reconstructed near-surface wind speeds at 10 m from both MENA CORDEX and MERRA-2 as the reference height wind speeds and assume that $\alpha = 1/7$, as it is appropriate over open land surfaces and used in prior studies on wind in Saudi Arabia (Rehman et al., 2007; Tagle et al., 2017). Further, we assume that the air density at MENA CORDEX locations situated in the neighborhood of a MERRA-2 location is equal to the air density at this MERRA-2 location. Using the interpolated air density, we compute WPDs at the finer CORDEX spatial resolution to investigate in more details the regional behavior of wind power potential in Saudi Arabia. We compute projected WPDs over the period 2025–2050 (26 years) based on the interpolated air density from the current 26-year period (i.e., 1980–2005), even though minor changes in air density might occur due to regional warming.

4. Temporal Variability of Spatially Averaged Wind Speeds

Here we focus on the time series of spatially averaged daily wind speeds over land. To analyze the variability in the annual cycle, we compute daily mean wind speeds (Figure S1 in the supporting information) and monthly mean wind speeds (Figure 2a) over the 26-year period 1980–2005, from the five CORDEX runs and three reanalysis products (i.e., MERRA, MERRA-2, and ERA-Interim). CORDEX simulations exhibit a significant negative bias in wind speeds when compared to MERRA and ERA-Interim, but a much smaller bias when compared to MERRA-2 during all months except for July and November when MERRA-2 and ERA-Interim present comparable monthly mean wind speeds. Analyses of the regional wind speed spatial and spatiotemporal patterns, shown in the next sections, also reveal that CORDEX is more similar to MERRA-2 than to ERA-Interim. Because of the higher degree of agreement between MERRA-2 and MENA CORDEX outputs—likely as a result of the advancements in data assimilation with respect to MERRA and ERA-Interim—we use MERRA-2 as the reference in all our evaluation analyses. The mean of spatially averaged wind speed calculated from MERRA-2 is approximately 3.5 m/s, while the one from the five ensemble runs of MENA CORDEX varies between 2.8 m/s and 3.1 m/s. Nevertheless, all five CORDEX simulations capture the seasonality or annual cycle patterns and heteroskedasticity in MERRA-2, showing a higher variability of wind speeds in winter and spring than in summer and fall.

To examine which CORDEX run performs the best against MERRA-2 mean wind speeds, we apply Taylor diagrams to spatially averaged monthly mean and seasonal mean wind speeds from the two data sets

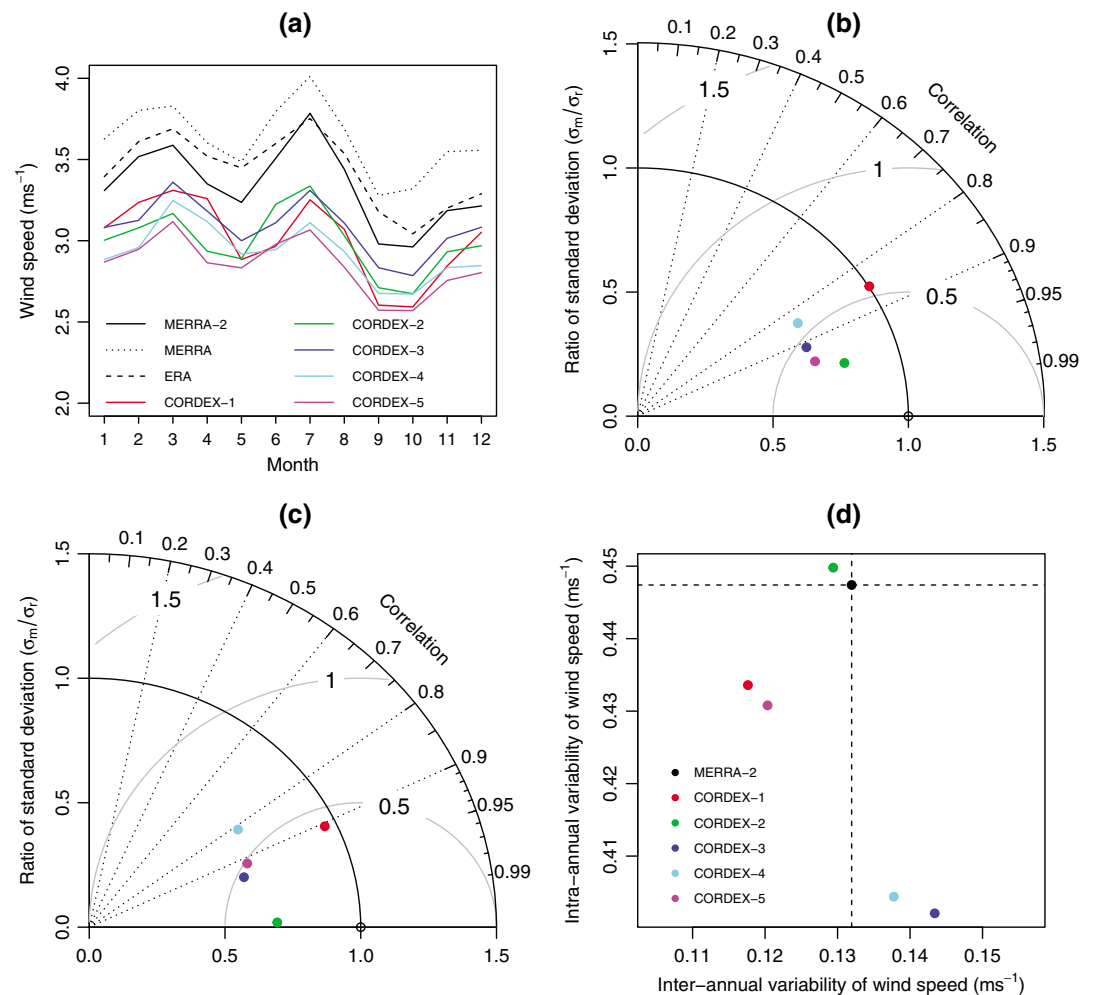


Figure 2. (a) Annual cycle of monthly mean wind speed (m/s); Taylor diagrams of (b) monthly mean and (c) seasonal mean wind speeds (m/s) from spatially averaged data for MERRA, ERA-Interim, MERRA-2, and the five CORDEX runs, temporally averaged during 1980–2005. In the Taylor diagrams, MERRA-2 is used as the reference. (d) Interannual and intra-annual variabilities of wind speed from MERRA-2 and the five CORDEX runs during 1980–2005. The dashed lines represent metrics for MERRA-2. MERRA-2 = Modern Era Retrospective-Analysis for Research and Applications version 2; CORDEX = Coordinated Regional Climate Downscaling Experiment.

(Figures 2b and 2c). In both cases, CORDEX-2 shows the highest agreement with MERRA-2, having a similar standard deviation, the highest correlation coefficient (>0.97), and the lowest RMSD. CORDEX-2 is simulated by applying RCA4 and is driven by the EC-EARTH model under a spatial resolution of 0.44° (latitude/longitude).

Wind fields fluctuate on different time scales such as daily, monthly, seasonal, and yearly. Thus, besides assessing their climatology, it is also important to quantify their temporal variability. We first assess the interannual and intra-annual variabilities of spatially averaged wind speeds from MENA CORDEX and MERRA-2 over land areas for the period 1980–2005. The interannual variability is defined as the standard deviation of annual mean wind speed among different years, and the intra-annual variability is defined as the standard deviation of monthly mean wind speed among different months (Chen et al., 2012; Pryor, Barthelmie, & Schoof, 2012). As we can see from Figure 2d, all MENA CORDEX simulations, except for CORDEX-2, underestimate the intra-annual (or monthly) variability, compared to MERRA-2. CORDEX-2 shows the smallest distance to MERRA-2, which implies that it best captures MERRA-2's temporal variability. For wind power considerations, it is also important to reproduce the extreme winds (e.g., 95% quantile) in addition to the mean wind fields. However, since the extreme winds present higher uncertainties and variabilities over the study region with such a complex topography, averaging over the whole domain will neglect the significant regional variability. In fact, the Taylor diagram of 95% quantile wind speed averaged over land areas (not reported) indicates that

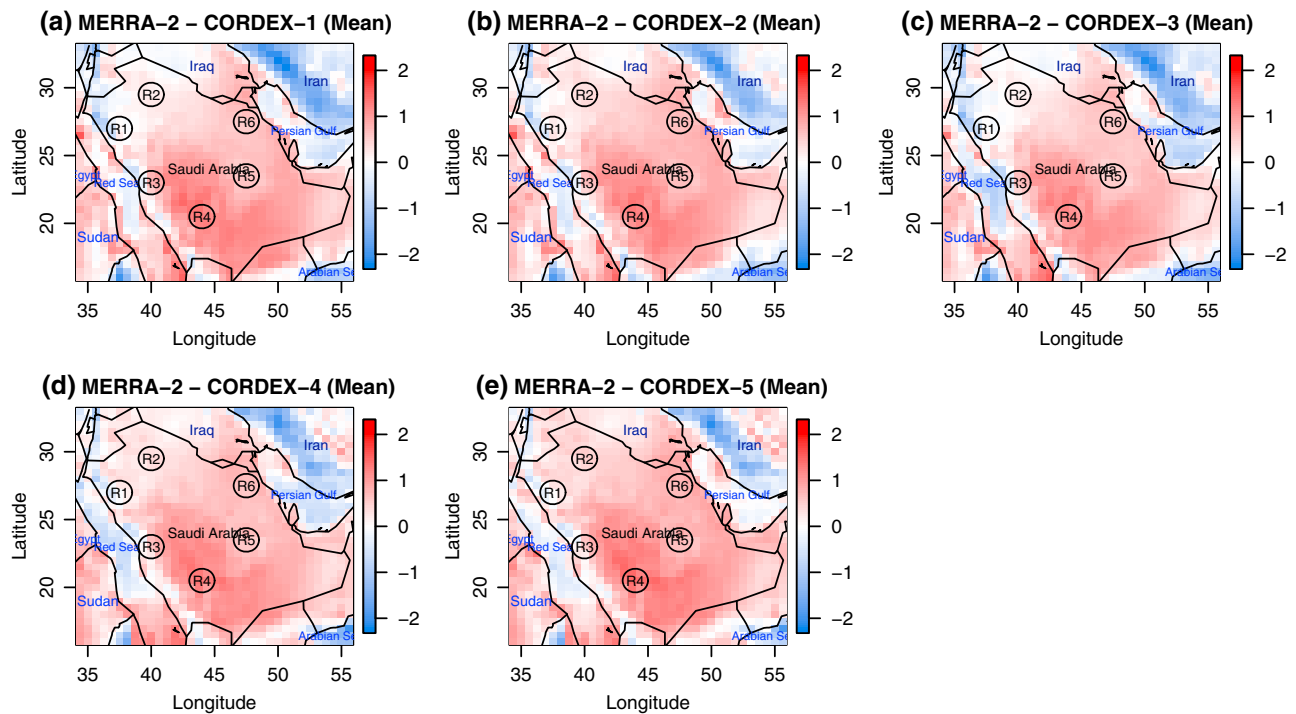


Figure 3. Difference in mean wind speed (m/s) between MERRA-2 and each of the five MENA CORDEX runs during 1980–2005. Cold colors indicate a positive bias in the model (i.e., the mean is larger for CORDEX than for MERRA-2); warm colors show where the model is negatively biased in relation to MERRA-2. White corresponds to 0 (i.e., no difference between MERRA-2 and CORDEX). MERRA-2 = Modern Era Retrospective-Analysis for Research and Applications version 2; CORDEX = Coordinated Regional Climate Downscaling Experiment.

the five CORDEX runs perform almost equally poorly when comparing to MERRA-2. This issue from averaging over space is not that severe for the monthly mean and seasonal mean wind speeds (as shown in Figures 2b and 2c) due to the inherent seasonality of the wind climate. Instead, we have investigated the extreme winds (1-, 5-, 10-, and 30-year return levels) over the six selected regions (see section 5) in order to examine the ability of CORDEX runs in capturing regional extreme wind climatology.

Finally, the comparison among three different reanalysis data sets—MERRA, MERRA-2, and ERA-Interim (Figure 2a)—also implies that the biases are more likely to be negative biases in the CORDEX model results and that the bias is higher when comparing to ERA-Interim and MERRA than MERRA-2. A more thorough evaluation is limited due to the lack of direct observations over the study region.

5. Spatial Variability of Wind Speed Mean, Variance, Quantiles, and Return Levels

We compute the mean, standard deviation, and quantiles of the wind speed time series from MERRA-2 and CORDEX, for the period 1980–2005 at each location in the region of interest. The mean wind speeds are highly consistent within the five CORDEX runs (Figure S2) and show a negative bias for all locations except for the regions adjacent to the Red Sea. For these regions, we find the bias to be close to zero, whereas the bias is positive over most sea areas and western Iran (Figure 3). Similar results are found for the standard deviation (Figure S3), the median (or 50% quantile), and the 95% quantile of wind speeds (not reported).

Here again, we use the Taylor diagram to quantify the ability of each CORDEX run to capture MERRA-2 spatial patterns. As indicated in Figure S4, the skills of the five MENA CORDEX runs in simulating MERRA-2 spatial fields of temporally averaged mean, standard deviation, median, and 95% quantile are quite similar. Since the three statistical metrics in the Taylor diagram provide an overall assessment of model skills at all locations within the study region, a higher model performance over specific regions might be offset and lead to an apparent similar performance of the five CORDEX runs in relation to MERRA-2. Therefore, we assess the model's performance over the six regions selected in section 2 (see Figures 4a and 4b). Although no run shows a uniformly higher performance in capturing spatial patterns over all six regions, CORDEX-4 appears to outperform the other runs. Specifically, CORDEX-4 has the highest skills in simulating mean wind speeds for Regions R5 and R6,

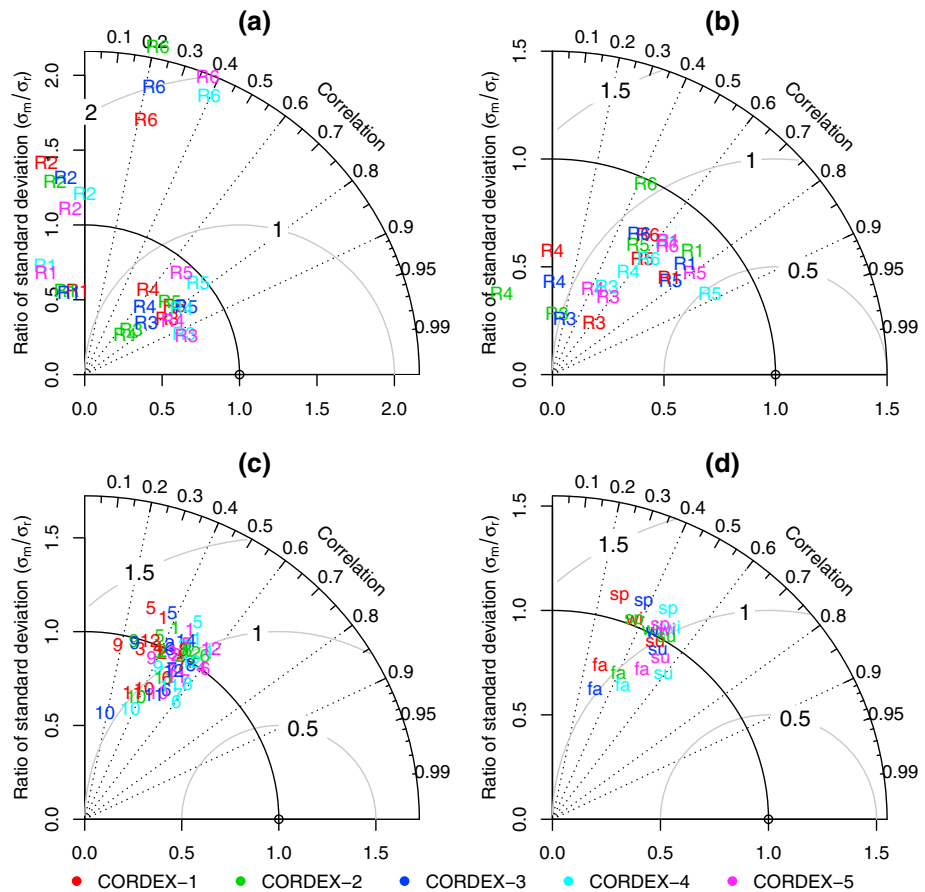


Figure 4. Taylor diagrams for the spatial fields of (a) mean wind speeds and (b) wind speed standard deviations, over the six selected regions (indicated as R1–R6), (c) monthly mean wind speed (with numbers indicating the corresponding month), and (d) seasonal mean wind speed (with “wi,” “sp,” “su,” and “fa” indicating winter, spring, summer and fall, respectively) for the five CORDEX runs (in different colors). MERRA-2 is used as the reference. Region 2 (R2) is not shown in Figure 4b because its values are significantly different from the others. MERRA-2 = Modern Era Retrospective-Analysis for Research and Applications version 2; CORDEX = Coordinated Regional Climate Downscaling Experiment.

located in the east part of Saudi Arabia, and in simulating wind speed variability for Regions R2, R4, and R5, located in the north, south, and east, respectively. We should note that CORDEX-5 has an ability to simulate mean wind speeds for R3 (located between Yanbu and Mecca) and R4 (located east of the Asir Mountains) that is comparable to CORDEX-4, and it outperforms CORDEX-4 in wind speed variability for R6 (located near the Persian Gulf). All CORDEX runs exhibit a high ability to reproduce mean wind speeds over the R3, R4, and R5 regions located in the south. Further, they show good skills in capturing the wind speed variability for the R1 and R5 regions located in the northwest and east, respectively. In contrast, all five CORDEX runs perform poorly in simulating winds over R2, located in the north, near the city of Sakaka. Especially for wind speed standard deviations over R2, they exhibit low correlation coefficients (between 0.1 and 0.2), high standard deviation ratios, and high proportional distances of RMSDs (both are between 2 and 3) in relation to MERRA-2 (not shown in the figure). With respect to the mean wind speeds, all CORDEX runs present negative correlation coefficients with MERRA-2 in R1 (in the northwest and close to the Red Sea) and R2 (in the north).

In our study, we also report the spatial fields of the 5-year return levels of near-surface wind speeds (Figure 5). The 5-year return levels that are computed from MERRA-2 are higher than those computed from CORDEX simulations over most regions in Saudi Arabia, except for the coastal Red Sea region. One exception is CORDEX-4, which exhibits higher values than those from MERRA-2 in the southeast region of Saudi Arabia between the Persian Gulf and Arabian Sea. We obtain similar results for 1-, 10-, and 30-year return levels (not shown).

To measure the degree of agreement between the five CORDEX runs and the MERRA-2 return levels, we analyze the Taylor diagrams (not shown) for their spatial fields over the land areas in the whole study domain.

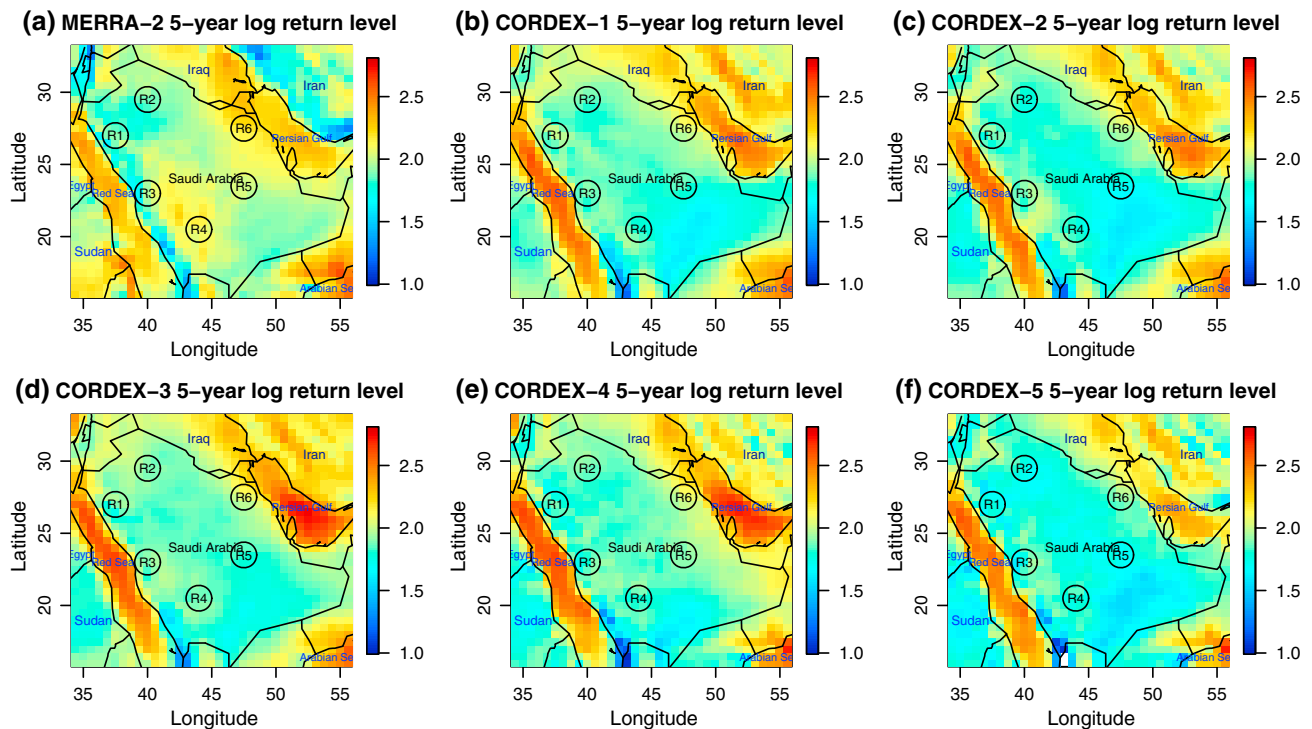


Figure 5. The 5-year log return levels of wind speed (m/s) from the five CORDEX runs (b–f) and MERRA-2 (a). MERRA-2 = Modern Era Retrospective-Analysis for Research and Applications version 2; CORDEX = Coordinated Regional Climate Downscaling Experiment.

For the 1-, 5-, and 10-year return levels, correlation coefficients between simulations and reanalysis are ~ 0.35 , standard deviation ratios are close to 1, and the proportional distances of RMSDs are between 1 and 1.5. Although the five CORDEX runs exhibit a similar performance, CORDEX-4 shows slightly higher skills in reproducing MERRA-2 return levels. The model performance worsens as the return period increases, due to a higher uncertainty caused by a higher quantile of extreme wind speeds. We further investigate the model performance in capturing wind speed return levels over the six regions (Figure S5). CORDEX-4 outperforms the other runs in most cases, and the CORDEX runs have the highest skills in estimating return levels over R3, located inland the Red Sea coast, between the cities of Yanbu and Mecca. Additionally, all CORDEX runs perform poorly for the R2, located near the northern city of Sakaka, and for R4, located east of the Asir Mountains.

From the spatial analysis, we can conclude that the five CORDEX simulations exhibit a negative bias—relative to MERRA-2—in mean, standard deviations, median, and 95% quantile of wind speeds, as well as the 1-, 5-, 10-, and 30-year return levels, for almost all locations in Saudi Arabia, except the region near the coastline of the Red Sea (where it is close to zero). The bias is positive, however, for sea areas including the Red Sea, the Persian Gulf, and the Arabian Sea. Based on the Taylor diagrams, we conclude that the five CORDEX runs have almost the same ability to simulate wind speed spatial patterns over the whole domain of study in relation to MERRA-2. CORDEX-4 (which is driven by the GFDL-ESM2M model under a spatial resolution of 0.22° latitude/longitude) appears to perform slightly better than the other CORDEX runs. When considering regional performances over the six selected regions, CORDEX-4 exhibits significantly higher skills than the other runs in most cases, and CORDEX-5 (which is driven by the EC-EARTH model under a spatial resolution of 0.22° latitude/longitude) presents comparable or even higher skills than CORDEX-4 in a few cases only. The higher performance of CORDEX-4 and CORDEX-5 in capturing the spatial variability and regional behavior of wind climatology may be the result of the applied finer spatial resolution in CORDEX-4 and CORDEX-5 than in the other runs.

For comparison, we conduct similar analyses on the spatial fields using ERA-Interim as the reference (the figures are not reported due to the paper length constraints). Results from these analyses indicate that the difference (in absolute value) in mean wind speed with CORDEX is higher for ERA-Interim than for MERRA-2. Further, the wind speed standard deviation from ERA-Interim (MERRA-2) is lower (higher) than that from the CORDEX runs over most regions in Saudi Arabia, possibly due to the coarser spatial resolution of ERA-Interim.

Further, the Taylor diagrams of the spatial fields of mean, standard deviation, and quantiles of wind speeds indicate that the agreement between ERA-Interim and CORDEX is lower than the one between MERRA-2 and CORDEX.

6. Wind Spatiotemporal Patterns

6.1. Annual Cycle of Wind Speeds Over Saudi Arabia

In order to examine the similarity between CORDEX simulations and MERRA-2 in describing the spatiotemporal behavior of wind speeds over Saudi Arabia for the 1980–2005 period, we analyze the annual cycle and seasonality at each location or regions of interest, instead of considering the spatial averages, as done in section 4. We compute the monthly and seasonal mean wind speeds over 26 years, at each location, and then use the Taylor diagram to assess the level of agreement between each of the five CORDEX runs and MERRA-2 spatial fields (Figures 4c and 4d). We find that CORDEX-4 performs the best in January, August, September, and December, whereas CORDEX-5 performs the best in February, April, May, October, and November, and that these two runs also outperform the other runs in March, June, and July. With respect to the seasonal mean wind speeds, CORDEX-4 outperforms the other runs in winter and summer, while CORDEX-5 outperforms the other runs in spring and fall. The five CORDEX runs have the highest skills during the summer months of June, July, and August (JJA), when the correlation coefficients are between 0.5 and 0.6, the ratios of standard deviations close to one, and the RMSDs relatively low. CORDEX runs exhibit lower skills in May, September, and October, when the correlation coefficients are quite low, the standard deviation ratios far from one, or the RMSDs high.

6.2. Temporal Wind Speed Variability Over Six Regions in Saudi Arabia

We have identified CORDEX-2 as the run with the best performance in reproducing MERRA-2 annual or seasonal wind speed patterns, and CORDEX-4 as the run with the best performance in simulating MERRA-2 spatial and regional wind speed patterns. Hence, in this section, we use CORDEX-2 and CORDEX-4 for analyzing the temporal evolution of wind speeds over the six selected regions, using MERRA-2 as the reference. We compute the monthly means of daily wind speeds for each of the 26 years over the 1980–2005 period and display the results for the six regions using functional boxplots (Figure S6). Note that in the functional boxplot, the central curve represents the median, the shaded band is the 50% central region envelope, the band bounded by the outer curves is the maximum nonoutlying envelope, and the dashed curves are potential outliers. This analysis highlights discrepancies in the annual cycle patterns, over the six regions, between MERRA-2 and CORDEX-2/4. For example, winds in R1 (northwest and close to the Red Sea) from MERRA-2 exhibit peaks in summer and lows in winter, a pattern also found in the R6 (north and close to the Persian Gulf) based on CORDEX-2/4. On the other hand, R6 from MERRA-2 shows lower seasonal fluctuations, similar to what we obtained with CORDEX-2/4 for the R1. As for R2 (in the north), MERRA-2 shows strong winds in middle spring, whereas CORDEX-2/4 show a peak in December (with CORDEX-4 wind speeds even higher than those from MERRA-2 during the winter). Furthermore, CORDEX-2 and CORDEX-4 exhibit different skills with respect to MERRA-2, in specific regions. For instance, CORDEX-2 can better capture the MERRA-2 temporal trends than CORDEX-4 in R3 (in the west and close to the Red Sea) where winds are strongest in summer, but CORDEX-4 is able to reproduce the wind temporal variability (shown by the bandwidth of the 50% central region) of MERRA-2 in R2 (northern region). The comparison of spatiotemporal wind patterns between CORDEX and ERA-Interim indicates that all CORDEX runs have quite low degree of agreement with ERA-Interim, and no run performs uniformly better than the others. Only CORDEX-2 shows higher skills in reproducing mean wind speed over Regions 3 and 6 (figures not reported due to length constraints).

7. Wind Energy Potential in Saudi Arabia

The analyses presented in sections 4–6 show that CORDEX-4, which has higher spatial resolution, better captures MERRA-2's wind spatial and regional patterns than CORDEX-2; however, this apparent improvement is lost when performing spatial aggregation. Furthermore, when analyzing spatiotemporal wind speed patterns, CORDEX-2 and CORDEX-4 exhibit different performances depending on the month or season of the year and the region considered. This suggests that different CORDEX runs should be adopted to assess the wind power potential depending on the research focus, that is, WPD temporal, spatial, or spatiotemporal patterns. In this section, we compute WPDs over Saudi Arabia for the current period (i.e., 1980–2005), based on both MERRA-2 and CORDEX-2/4 data sets to investigate whether or not the wind resource characterization

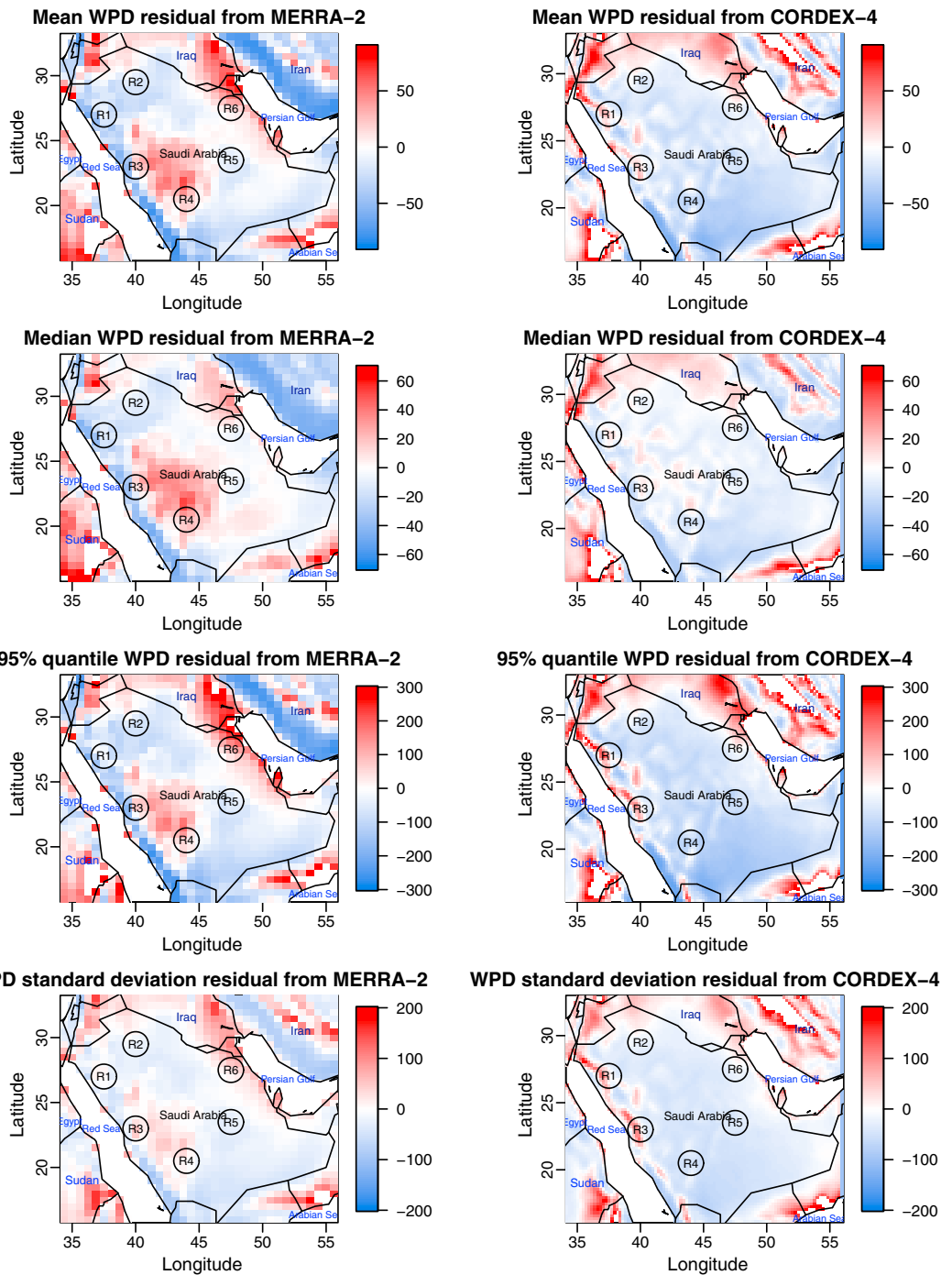


Figure 6. Residuals of mean, median, 95% quantile, and standard deviation of WPD (W/m^2) at 80 m computed from MERRA-2 (left) and CORDEX-4 (right) using the power law method during 1980–2005. MERRA-2 = Modern Era Retrospective-Analysis for Research and Applications version 2; CORDEX = Coordinated Regional Climate Downscaling Experiment; WPD = wind power density.

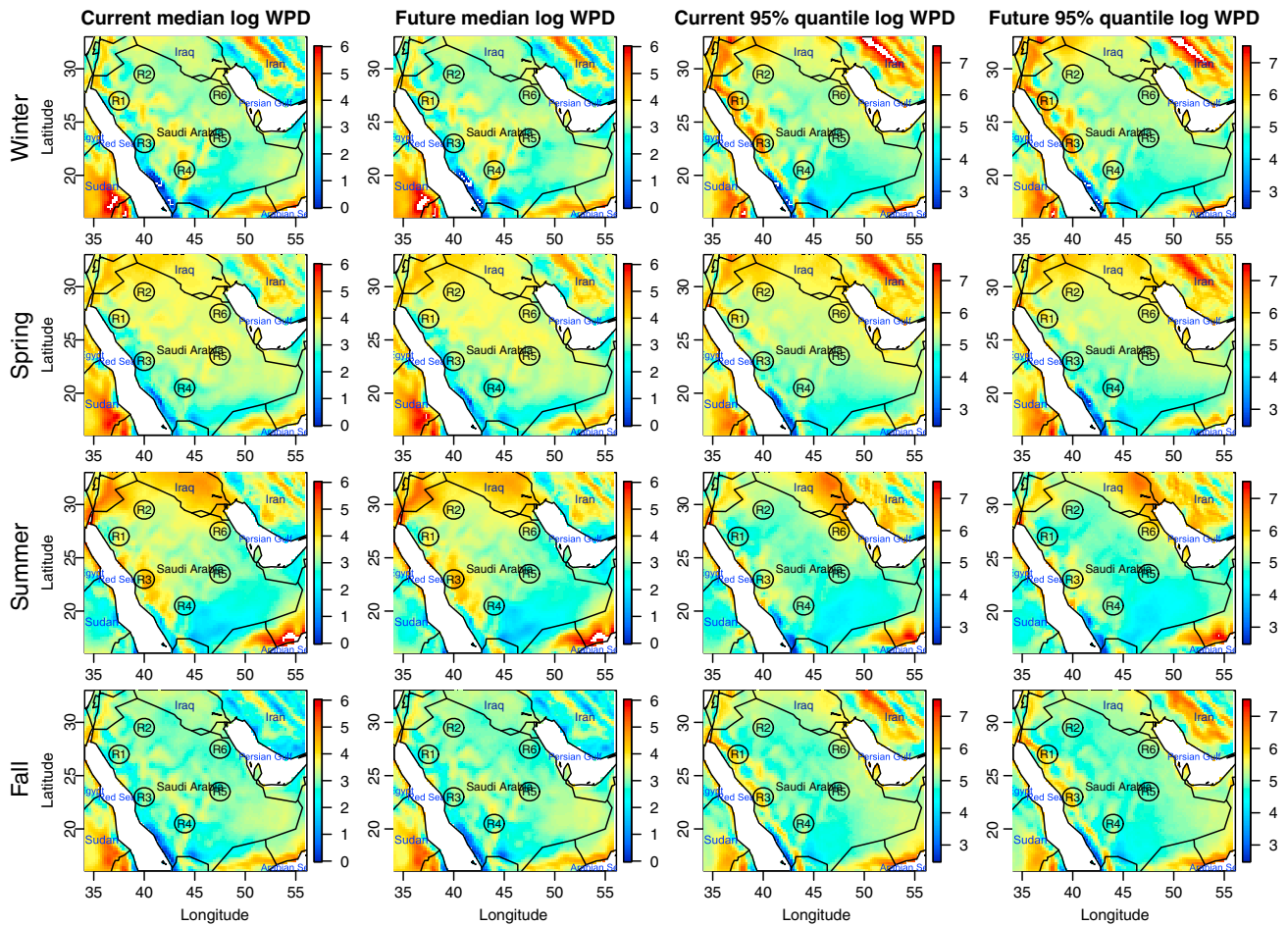


Figure 7. Median (the first two columns) and 95% quantile (last two columns) of log WPD (W/m^2) by seasons (on different rows) for the current period (1980–2005, first and third columns) and in the future (2025–2050, second and fourth columns) from CORDEX-4. CORDEX = Coordinated Regional Climate Downscaling Experiment; WPD = wind power density.

shows any significant discrepancy between the two data sets. In addition, since projections are available from MENA CORDEX for the 2006–2100 period, we compute WPDs for the future 2025–2050 period to make inference about potential changes in projected wind resources. Based on our previous findings, we use CORDEX-4 to investigate the spatial patterns of WPDs and both CORDEX-2 and CORDEX-4 to analyze the temporal variability of WPDs over the six selected regions. These analyses can be instrumental in establishing where wind farms should be built, at present and future times when high WPDs are expected to occur.

7.1. Current and Future WPD Estimates

Since CORDEX-4 has the highest skills in simulating wind speed spatial patterns, we use its output to compute WPDs. We first interpolate the air density variable available in MERRA-2 for the current period 1980–2005 to the finer spatial resolution of CORDEX-4 (0.22° latitude/longitude), as described in section 3. Figure S7 shows the spatial fields of the mean, median, 95% quantile, and standard deviation of WPDs at 80 m, computed from MERRA-2 and CORDEX-4 for the period 1980–2005. WPDs computed from CORDEX-4 are generally smaller than those derived from MERRA-2. This is because CORDEX runs have a systematic negative bias of wind speeds, as discussed in sections 4–6. Thus, in order to identify possible discrepancies in the spatial variabilities of WPDs only, we ignore the difference in WPD magnitude and subtract the mean over space. The resulting residuals show a significant difference in WPD spatial variability between MERRA-2 and CORDEX-4 (Figure 6). Results from WPD computations using MERRA-2 show an abundant wind power potential over a vast region in the southwest, roughly bounded by longitude $41^\circ E$ – $45^\circ E$ and latitude $21^\circ N$ – $24^\circ N$. In this region,

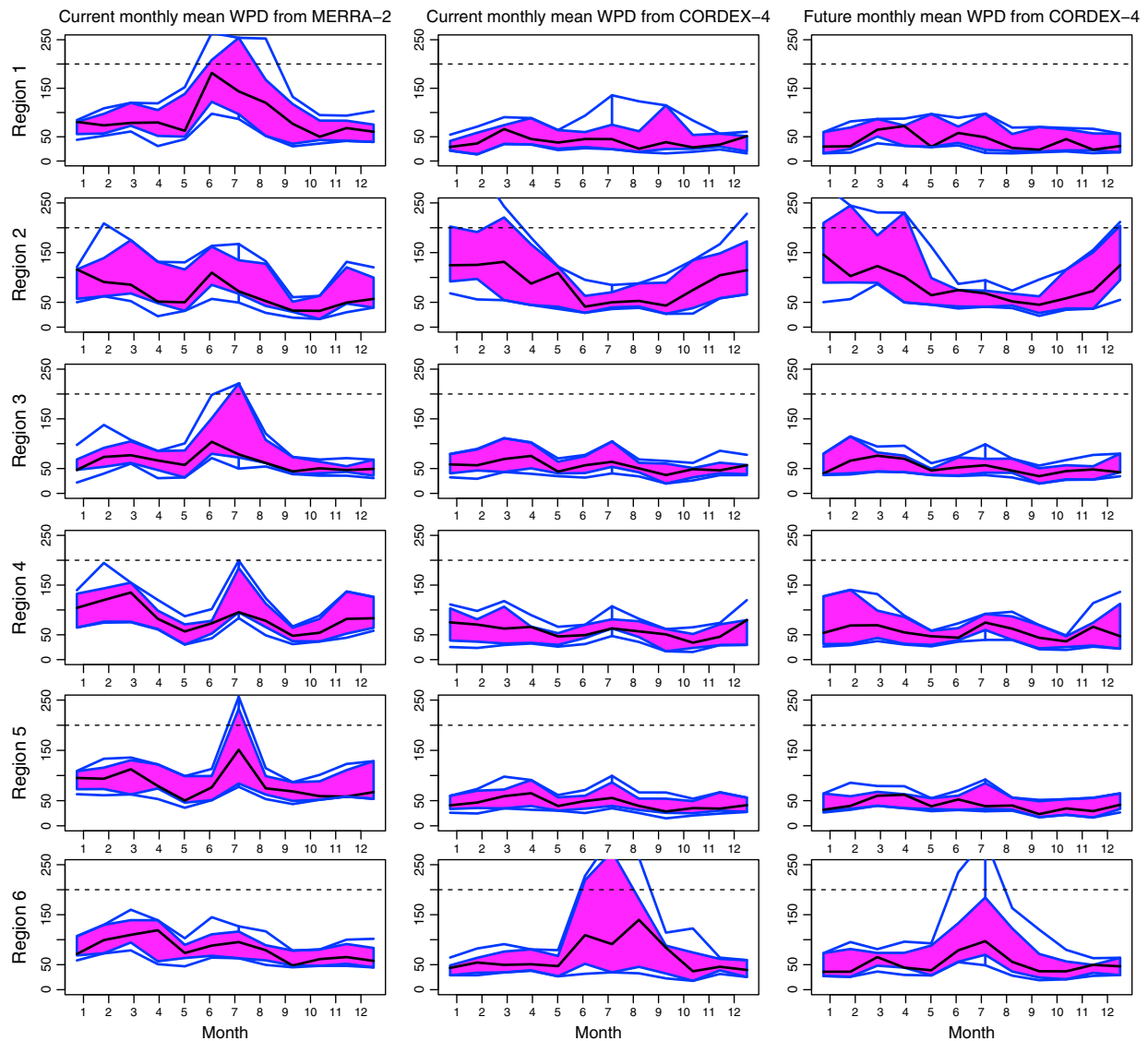


Figure 8. Functional boxplots for the 26 time series of monthly mean WPD (W/m^2) from MERRA-2 (left) and CORDEX-4 (center), in the current period (1980–2005). The right column shows WPD from CORDEX-4 in the future period (2025–2050) for each of the six regions. The dashed lines indicate the 200 W/m^2 WPD threshold. MERRA-2 = Modern Era Retrospective-Analysis for Research and Applications version 2; CORDEX = Coordinated Regional Climate Downscaling Experiment; WPD = wind power density.

the mean WPD is $\sim 150 \text{ W/m}^2$ and the 95% quantile can reach up to 500 W/m^2 . These values are comparable to those obtained by Yip et al. (2016). Wind energy potential can be also found in areas adjacent to the Persian Gulf. However, abundant wind power is identified by CORDEX-4 at only a limited number of locations, mostly in areas close to the Red Sea.

When comparing to ERA-Interim, the residual maps of mean, median, 95% quantile, and standard deviation of WPD (not reported), the spatial fields of ERA-Interim WPD appear quite different from those of CORDEX-4: similar to MERRA-2, ERA-Interim exhibits high WPD over a vast area in west Saudi Arabia between Regions 3 and 4, but ERA-Interim differs more from CORDEX-4 by exhibiting high WPD over north Saudi Arabia.

We now quantify the wind energy resources in the future (years 2025–2050) to detect possible changes in the wind power potential. In Figure 7, CORDEX-4 projections show abundant wind resources over west Saudi Arabia between R1 and R4 in winter but only moderate resources over a vast region in the north during spring. The areas close to the Red Sea and surrounding R3 (between Yanbu and Mecca) exhibit a high-energy

potential in summer, and the wind resource is the least abundant in most areas during fall. Based on the 95% quantile of WPD, however, Red Sea shores seem to have a high potential for wind energy in all seasons except spring, during which moderate WPDs are identified mainly in the north. Wind is extremely abundant in the northwest, between R1 and R3 (in the west and close to the Red Sea) during winter, with a 95% quantile higher than 500 W/m². On the other hand, only a limited number of locations in the west and close to the Red Sea exhibit a high wind power potential during summer and fall. We also observe high WPDs in summer over R6, which is close to the Persian Gulf. By comparing WPD maps for the current and future periods, we find that WPD projections are highly consistent with current estimates. Hence, building wind farms at locations with high wind power potential for both current and future wind harvesting should be strongly considered.

To analyze the temporal behavior of WPD over the six regions, we use both CORDEX-2 (Figure S8) and CORDEX-4 (Figure 8). A threshold of 300 W/m² (Wind Class 3) for WPD was proposed to identify sites for commercial scale power production in the Regional Energy Deployment System model of the National Renewable Energy Laboratory (Short et al., 2011). Yip et al. (2016) have adopted a lower threshold of 200 W/m² (Wind Class 2) to quantify wind power availability, due to the recent developments in low wind turbines. We also indicate the 200 W/m² threshold in Figures S8 and 8. The temporal variabilities of contemporary WPDs for MERRA-2 and the two CORDEX runs are quite different over the selected regions. For example, in R1 (in the northwest and close to the Red Sea), MERRA-2 shows extremely abundant wind resources in summer, but CORDEX-2/4 only indicate moderate WPDs (all below the threshold) in this region during the entire year. In R2 (in the north), CORDEX-2/4 show the highest WPDs during late winter and early spring, which are usually higher than those from MERRA-2. In R6 (near the Persian Gulf), CORDEX-2/4 show abundant wind resources in summer, but MERRA-2 presents less volatile WPDs that are all below the threshold. Moreover, WPDs in R4 and R5 (in the east) indicate a systematic negative bias of CORDEX-2/4 relative to MERRA-2 both in the magnitude and temporal variabilities. In R3 (in the west and close to the Red Sea) and R5 (in the east), MERRA-2 reveals WPD above the threshold in July, whereas CORDEX-2/4 exhibit WPDs significantly below the threshold. High wind energy potentials in CORDEX-2/4 over their respective regions tend to persist from current to future climates, as highlighted by the functional boxplots of current and future mean WPDs.

8. Model Biases and Performance Discrepancies

Here we investigate possible sources of model biases and discrepancies against a target and discuss the associated implications for wind energy potential assessment. As shown in Figure 2a, the difference between CORDEX and MERRA-2 is as large as about 10% even for the best scenario. This bias will be augmented by a cubic growth (as shown in equation (2)) when estimating the WPD, which is not negligible.

In regional climate simulations, a regional model is often tuned to have an optimal configuration over a specific spatial domain and thus to produce the most accurate results with respect to some observed data set (Kalognomou et al., 2013). Simulated results may be sensitive to the size and topography of the domain, the choice of RCM, the initial conditions, the lateral boundary conditions or the choice of driving ESMs, temporal/horizontal/vertical resolutions, and physical parameterization schemes. There have been many diagnostic studies on how these factors can introduce intermodel or intramodel variabilities as well as systematic biases of simulated climate variables in an RCM, such as precipitation and surface temperature (see, e.g., Cr  tat & Pohl, 2012; Kalognomou et al., 2013; Zittis & Hadjinicolaou, 2017). Some studies have sought to attribute the sources of bias in wind speeds from regional climate simulations, although none of them focused on the MENA region. Effects of initial/boundary conditions, spatial resolutions, and adopted parameterizations on regionally simulated winds were investigated, for example, in Borge et al. (2008), Carvalho et al. (2012), Chen et al. (2012), Pryor, Barthelmie, and Schoof (2012), Pryor, Nikulin, and Jones (2012), and Carvalho et al. (2014). In this study, we have assessed the influence of lateral boundary conditions and spatial resolution on wind speeds from MENA CORDEX simulations by comparing the original runs against two additional MENA CORDEX evaluation runs driven by ERA-Interim. We have also included a comparison against ERA-Interim as an additional reanalysis product to investigate the magnitude of the model bias. Figure S9 shows the annual cycle of monthly mean wind speed from spatially averaged data and the temporal variabilities for MERRA, ERA-Interim, MERRA-2, and the CORDEX runs. Figures S9a and S9b compare CORDEX runs adopting the same spatial resolution but different boundary conditions and indicate that the magnitude of wind speeds from CORDEX evaluation runs fluctuates more throughout the year than those from the historical runs with the same spatial resolution. In this comparison the magnitude of the bias between CORDEX and the reanalysis

Table 2

Percentage Biases for CORDEX-2/4 With Respect to MERRA-2 in Mean Wind Speeds During 1980–2005, Averaged Over Each of the Six Selected Regions

Model run	Region 1	Region 2	Region 3	Region 4	Region 5	Region 6
CORDEX-2	−13.91	5.65	−1.46	−8.46	−26.06	−18.77
CORDEX-4	−11.51	8.84	−7.29	−14.39	−27.09	−19.44

products varies both depending on the driving ESM and the time of the year. Figures S9c and S9e compare CORDEX runs driven by the same ESM but adopting different spatial resolutions. Specifically, the evaluation run with higher spatial resolution is less biased relative to the reanalysis products throughout the year except for July and August, but the historical run driven by EC-EARTH with higher spatial resolution (CORDEX-4) is less biased than the run with lower spatial resolution (CORDEX-2) only in March, and the historical run driven by GFDL-ESM2M with higher spatial resolution (CORDEX-5) is much more biased than the run with lower spatial resolution (CORDEX-3) throughout the year. Also from Figures S9a–S9e, MERRA and ERA-Interim deviate even more from the CORDEX runs, except during July and November when ERA-Interim shows comparable monthly mean wind speeds with MERRA-2. From Figure S9f, the CORDEX evaluation run with higher spatial resolution (CORDEX22) shows a much lower intra-annual variability compared to the run with lower spatial resolution (CORDEX44), and the five CORDEX historical runs are more concentrated around MERRA-2 than around ERA-Interim or MERRA, with CORDEX-2 showing the best agreement with MERRA-2. In conclusion, the bias between MENA CORDEX simulations and the reanalysis data appears to be related to both the spatial resolutions applied and the driving lateral boundary conditions. Additional possible sources of model bias relate to the RCM and specific physical scheme choices. A more thorough assessment of the sources of the bias of simulated wind speeds over the MENA domain, which is characterized by a complex and diverse terrain and meteorology, including extended mountainous and coastal areas, as well as wide deserts, is certainly a relevant topic that will be part of future investigations in which higher-resolution simulations will be performed (e.g., by applying the Weather Research and Forecasting model).

To compensate for the systematic model biases, different approaches could be applied depending on the analyzed wind statistics (e.g., mean, standard deviation, high quantiles, and return periods). Further, the bias will vary both in space and time and additional uncertainties on the corrected WPD estimates will derive from the reanalysis products themselves. Here we investigate the spatial variability in model bias and quantify its impact on WPD estimates. For each of the six regions, we compute the percentage biases for the mean, standard deviation, median, and 95% quantile of wind speeds for the five CORDEX historical runs relative to MERRA-2 over the 26 years (i.e., 1980–2005, see Figure S10 in the supporting information). The biases for the mean wind speeds from CORDEX-2/4 are largest in regions of low winds (i.e., R5), and the absolute values of percentage biases in regions of high wind power potential (i.e., R3 and R4) are generally within 10% (Table 2). These results suggest that the mean WPD estimates would also be inflated should a bias correction be applied.

9. Conclusion and Discussion

Our work presents the first assessment of wind energy resources and associated spatiotemporal patterns over the entire Arabian Peninsula, based on evaluations using regional model runs from MENA CORDEX against the MERRA-2 reanalysis product. Results from our study indicate that the MENA CORDEX runs

1. capture the spatially averaged temporal (monthly and seasonal) patterns identified by the reanalysis data (even though they tend to underestimate the intra-annual variability), and that the highest wind speeds are identified during summer (when the models also have highest skills) and winter months;
2. present a systematic negative bias in reproducing the reanalysis wind speed magnitude over most of the Arabian Peninsula with the exception of the Red Sea coastline that shows a bias close to zero;
3. indicate similar spatial patterns, although the highest agreement with reanalysis data is found when the model is run at higher spatial resolution; and
4. identify high wind power potentials for different months or seasons depending on the region.

Saudi Arabia is characterized by regions of high WPD potential, mostly located along the Red Sea coast and over areas in the southeast and adjacent to the Persian Gulf. However, high wind energy potential can be also found in other regions during specific seasons. The analysis of an RCM output allows us to investigate

possible changes in wind resources as a result of climate change. Specifically to Saudi Arabia, we establish that, in future decades (up to 2050), based on CORDEX projections, these areas will consistently show a high WPD and thus may be good locations for harvesting wind as a source of energy.

This work represents a first and important step toward a comprehensive and extensive quantification of wind energy resources, based on RCM simulations, which is of particular value for countries lacking continuous, detailed, and accessible observational data. Our study also emphasizes the potential of using such models to infer spatiotemporal variations of wind resources under current and future climate conditions. Results from this study suggest that current regional simulations do not accurately reproduce the magnitude of wind speeds compared to reanalysis data, and that intermodel variability exists. A more accurate quantification of wind resources over the Arabian Peninsula may be achieved by performing regional model simulations at high spatial and temporal resolutions, which is part of our planned research using the Weather Research and Forecasting model. Future investigations will be also directed to further explore sources of model variability, including sensitivity on the adopted spatial resolution and boundary layer parameterizations that could significantly impact near-surface wind speeds.

Acknowledgments

Our work was supported by King Abdullah University of Science and Technology (KAUST)'s Office of Sponsored Research (OSR) under award OSR-2015-CRG4-2640. The MERRA-2 data used in this study were provided by the Global Modeling and Assimilation Office (GMAO) at the NASA Goddard Space Flight Center. MERRA-2 wind speed data (U_{10M} and V_{10M}) have been accessed from a subset of MERRA-2's 2d, 1-hourly, time-averaged, single-level diagnostics files (Global Modeling and Assimilation Office (GMAO), 2015a), and the air density data (RHOA) have been accessed from a subset of MERRA-2's 2d, 1-hourly, time-averaged, surface flux diagnostics file (Global Modeling and Assimilation Office (GMAO), 2015b). The ERA-Interim reanalysis data were produced by the European Centre for Medium-Range Weather Forecasts (ECMWF). ERA-Interim wind speed data (u_{10} and v_{10}) were accessed from the ERA-Interim archive version 2.0 (Berrisford et al., 2011) via the ECMWF WebAPI, the programmatic way of retrieving data from the archive. We acknowledge the World Climate Research Programme's Working Group on Regional Climate, and the Working Group on Coupled Modelling, former coordinating body of CORDEX and responsible panel for CMIP5. We also thank the Swedish Meteorological and Hydrological Institute (SMHI) for producing and making available their model output. We also acknowledge the Earth System Grid Federation infrastructure, an international effort led by the U.S. Department of Energy's Program for Climate Model Diagnosis and Intercomparison, the European Network for Earth System Modelling and other partners in the Global Organisation for Earth System Science Portals (GO-ESSP). MENA CORDEX wind speed data (uas and vas) were accessed from the Earth System Grid Federation (ESGF, Cinquini et al., 2014) search portal hosted by the Centre for Environmental Data Analysis (CEDA).

References

- Berrisford, P., Dee, D., Poli, P., Brugge, R., Fielding, K., Fuentes, M., et al. (2011). The ERA-Interim archive version 2.0. Shinfield Park, Reading.
- Borge, R., Alexandrov, V., Del Vas, J. J., Lumbrales, J., & Rodríguez, E. (2008). A comprehensive sensitivity analysis of the WRF model for air quality applications over the Iberian Peninsula. *Atmospheric Environment*, *42*(37), 8560–8574.
- Carvalho, D., Rocha, A., Gómez-Gesteira, M., & Santos, C. (2012). A sensitivity study of the WRF model in wind simulation for an area of high wind energy. *Environmental Modelling & Software*, *33*, 23–34.
- Carvalho, D., Rocha, A., Gómez-Gesteira, M., & Santos, C. S. (2014). Sensitivity of the WRF model wind simulation and wind energy production estimates to planetary boundary layer parameterizations for onshore and offshore areas in the Iberian Peninsula. *Applied Energy*, *135*, 234–246.
- Chen, L., Pryor, S., & Li, D. (2012). Assessing the performance of intergovernmental panel on climate change AR5 climate models in simulating and projecting wind speeds over China. *Journal of Geophysical Research*, *117*, D24102. <https://doi.org/10.1029/2012JD017533>
- Cinquini, L., Crichton, D., Mattmann, C., Harney, J., Shipman, G., Wang, F., et al. (2014). The Earth System Grid Federation: An open infrastructure for access to distributed geospatial data. *Future Generation Computer Systems*, *36*, 400–417.
- Cook, N. J. (1986). *Designers guide to wind loading of building structures. Part 1*. Stoneham, MA: Butterworth Publishers.
- Crétat, J., & Pohl, B. (2012). How physical parameterizations can modulate internal variability in a regional climate model. *Journal of the Atmospheric Sciences*, *69*(2), 714–724.
- Davison, A. C., & Smith, R. L. (1990). Models for exceedances over high thresholds. *Journal of the Royal Statistical Society. Series B (Methodological)*, *52*, 393–442.
- Dee, D. P., Uppala, S., Simmons, A., Berrisford, P., Poli, P., Kobayashi, S., et al. (2011). The ERA-Interim reanalysis: Configuration and performance of the data assimilation system. *Quarterly Journal of the Royal Meteorological Society*, *137*(656), 553–597.
- Ebert, E. E., Janowiak, J. E., & Kidd, C. (2007). Comparison of near-real-time precipitation estimates from satellite observations and numerical models. *Bulletin of the American Meteorological Society*, *88*(1), 47–64.
- Emeis, S. (2005). How well does a power law fit to a diabatic boundary-layer wind profile. *DEWI Magazine*, *26*, 59–62.
- Emeis, S. (2013). *Wind energy meteorology: Atmospheric physics for wind power generation*. Berlin, New York: Springer.
- Gelaro, R., McCarty, W., Suárez, M. J., Todling, R., Molod, A., Takacs, L., et al. (2017). The Modern-Era Retrospective Analysis for Research and Applications, version 2 (MERRA-2). *Journal of Climate*, *30*(14), 5419–5454.
- Gleckler, P. J., Taylor, K. E., & Doutriaux, C. (2008). Performance metrics for climate models. *Journal of Geophysical Research*, *113*, D06104. <https://doi.org/10.1029/2007JD008972>
- Global Modeling and Assimilation Office (GMAO) (2015a). MERRA-2 tavg1_2d_slv_Nx: 2d,1-Hourly, time-averaged, single-level, assimilation, single-level diagnostics V5.12.4, Greenbelt, MD, USA, Goddard Earth Sciences Data and Information Services Center (GES DISC). <https://doi.org/10.5067/VJAFPL11CSIV>, accessed [2017-09-18].
- Global Modeling and Assimilation Office (GMAO) (2015b). Global Modeling and Assimilation Office (GMAO)(2015), MERRA-2 tavg1_2d_flg_Nx: 2d, 1-hourly, time-averaged, single-level, assimilation, surface flux diagnostics V5.12.4, Greenbelt, MD, USA, Goddard Earth Sciences Data and Information Services Center (GES DISC). <https://doi.org/10.5067/7MCPBJ41YOK6>, accessed [2017-09-18].
- Google Developers (2017). Google Maps Elevation API Documentation. Retrieved from <https://developers.google.com/maps/documentation/elevation/intro>, accessed [2017-09-06].
- Haidvogel, D. B., Arango, H., Budgell, W. P., Cornuelle, B. D., Curchitser, E., Di Lorenzo, E., et al. (2008). Ocean forecasting in terrain-following coordinates: Formulation and skill assessment of the Regional Ocean Modeling System. *Journal of Computational Physics*, *227*(7), 3595–3624.
- Jones, C., Giorgi, F., & Asrar, G. (2011). The coordinated regional downscaling experiment: CORDEX—An international downscaling link to CMIP5. *CLIVAR exchanges*, *16*(2), 34–40.
- KA-CARE (2012). King Abdullah City for atomic and renewable energy: Building the renewable energy sector in Saudi Arabia (Report).
- Kalognomou, E.-A., Lennard, C., Shongwe, M., Pinto, I., Favre, A., Kent, M., et al. (2013). A diagnostic evaluation of precipitation in CORDEX models over southern Africa. *Journal of Climate*, *26*(23), 9477–9506.
- Kunz, M., Mohr, S., Rauthe, M., Lux, R., & Kottmeier, C. (2010). Assessment of extreme wind speeds from Regional Climate Models—Part 1: Estimation of return values and their evaluation. *Natural Hazards and Earth System Sciences*, *10*(4), 907–922.
- Kupiainen, M., Samuelsson, P., Jones, C., Jansson, C., Willén, U., Hansson, U., et al. (2011). Rossby Centre regional atmospheric model RCA4. Rossby Centre Newsletter, June.
- López-Pintado, S., & Romo, J. (2009). On the concept of depth for functional data. *Journal of the American Statistical Association*, *104*(486), 718–734.
- Lu, X., McElroy, M. B., & Kiviluoma, J. (2009). Global potential for wind-generated electricity. *Proceedings of the National Academy of Sciences of the United States of America*, *106*(27), 10,933–10,938.

- New, M., Lister, D., Hulme, M., & Makin, I. (2002). A high-resolution data set of surface climate over global land areas. *Climate Research*, 21(1), 1–25.
- Pryor, S., Barthelmie, R., & Kjellström, E. (2005). Potential climate change impact on wind energy resources in northern Europe: Analyses using a regional climate model. *Climate Dynamics*, 25(7-8), 815–835.
- Pryor, S., Barthelmie, R., & Schoof, J. T. (2012). Past and future wind climates over the contiguous USA based on the North American Regional Climate Change Assessment Program model suite. *Journal of Geophysical Research*, 117, D19119. <https://doi.org/10.1029/2012JD017449>
- Pryor, S., Nikulin, G., & Jones, C. (2012). Influence of spatial resolution on regional climate model derived wind climates. *Journal of Geophysical Research*, 117, D03117. <https://doi.org/10.1029/2011JD016822>
- Rasmussen, D., Holloway, T., & Nemet, G. (2011). Opportunities and challenges in assessing climate change impacts on wind energy—A critical comparison of wind speed projections in California. *Environmental Research Letters*, 6(2), 024008.
- Rehman, S., & Ahmad, A. (2004). Assessment of wind energy potential for coastal locations of the Kingdom of Saudi Arabia. *Energy*, 29(8), 1105–1115.
- Rehman, S., El-Amin, I., Ahmad, F., Shaahid, S., Al-Shehri, A., & Bakhshwain, J. (2007). Wind power resource assessment for Rafha, Saudi Arabia. *Renewable and Sustainable Energy Reviews*, 11(5), 937–950.
- Rienecker, M. M., Suarez, M. J., Gelaro, R., Todling, R., Bacmeister, J., Liu, E., et al. (2011). MERRA: NASA's Modern-Era Retrospective Analysis for Research and Applications. *Journal of Climate*, 24(14), 3624–3648. <https://doi.org/10.1175/JCLI-D-11-00015.1>
- Saha, S., Moorthi, S., Pan, H.-L., Wu, X., Wang, J., Nadiga, S., et al. (2010). The NCEP climate forecast system reanalysis. *Bulletin of the American Meteorological Society*, 91(8), 1015–1057.
- Schmidt, G. A., Ruedy, R., Hansen, J. E., Aleinov, I., Bell, N., Bauer, M., et al. (2006). Present-day atmospheric simulations using GISS ModelE: Comparison to in situ, satellite, and reanalysis data. *Journal of Climate*, 19(2), 153–192.
- Shaahid, S., Al-Hadhrami, L. M., & Rahman, M. (2014). Potential of establishment of wind farms in western province of Saudi Arabia. *Energy Procedia*, 52, 497–505.
- Short, W., Sullivan, P., Mai, T., Mowers, M., Uriarte, C., Blair, N., et al. (2011). Regional Energy Deployment System (ReEDS) (Tech. Rep.). Golden, CO: National Renewable Energy Laboratory (NREL).
- Sun, Y., & Genton, M. G. (2011). Functional boxplots. *Journal of Computational and Graphical Statistics*, 20(2), 316–334.
- Tagle, F., Castruccio, S., Crippa, P., & Genton, M. G. (2017). Assessing potential wind energy resources in Saudi Arabia with a skew-t distribution. *arXiv preprint arXiv:1703.04312*.
- Taylor, K. E. (2001). Summarizing multiple aspects of model performance in a single diagram. *Journal of Geophysical Research*, 106(D7), 7183–7192.
- Taylor, K. E., Stouffer, R. J., & Meehl, G. A. (2012). An overview of CMIP5 and the experiment design. *Bulletin of the American Meteorological Society*, 93(4), 485–498. <https://doi.org/10.1175/BAMS-D-11-00094.1>
- van Vuuren, D. P., Edmonds, J., Kainuma, M., Riahi, K., Thomson, A., Hibbard, K., et al. (2011). The representative concentration pathways: An overview. *Climatic Change*, 109(1), 5. <https://doi.org/10.1007/s10584-011-0148-z>
- Yip, C. M. A., Gunturu, U. B., & Stenchikov, G. L. (2016). Wind resource characterization in the Arabian Peninsula. *Applied Energy*, 164, 826–836.
- Zhou, Y., Luckow, P., Smith, S. J., & Clarke, L. (2012). Evaluation of global onshore wind energy potential and generation costs. *Environmental Science & Technology*, 46(14), 7857–7864.
- Zittis, G., & Hadjinicolaou, P. (2017). The effect of radiation parameterization schemes on surface temperature in regional climate simulations over the MENA-CORDEX domain. *International Journal of Climatology*, 37(10), 3847–3862.